TOPICAL SYMPOSIUM on

Frontiers in Imaging Science: High Performance Nuclear Medicine Imagers for Vascular Disease Imaging (Brain and Heart)

Recent Advances in small animal PET instrumentation and techniques

Alberto Del Guerra
Department of Physics and INFN, Pisa,Italy
alberto.delguerra@df.unipi.it
www.df.unipi.it/~fiig

PET detectors detect the "back-to-back" photons (511 keV) produced during the *annihilation* process.

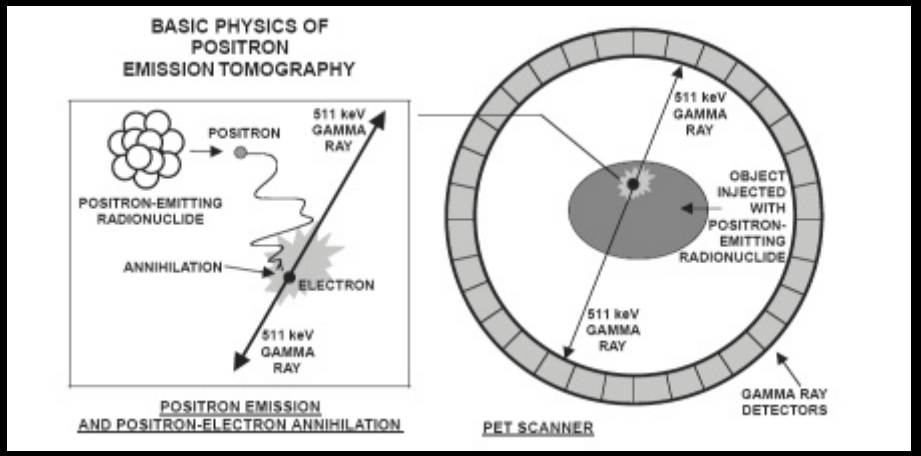

PET basic physics: β^+ decay

$$ {}^{A}_{Z}X_{N} \rightarrow {}^{A}_{Z-1}Y_{N+1} + e^{+} + \nu_{e} $$

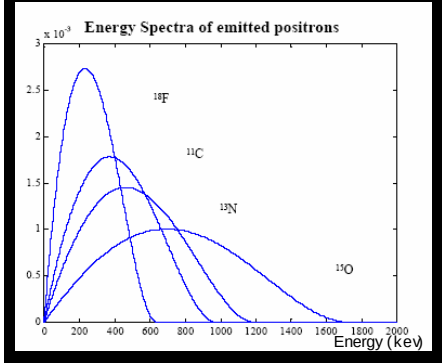

Kinetic energy balance:

$$ E_T = E_{b^+} + E_n + E_n $$

Nuclide	Max. β^+ energy (keV)	β^+ range in tissue (mm)
^{11}C	970	4.1
^{13}N	1190	5.1
^{15}O	1730	7.3
^{18}F	640	2.4

- PET scanning does not detect positrons: **range too short.**

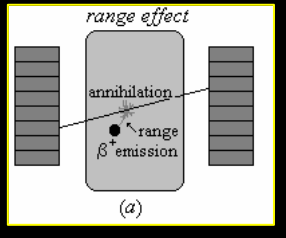

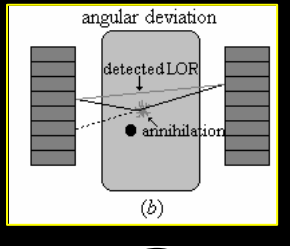

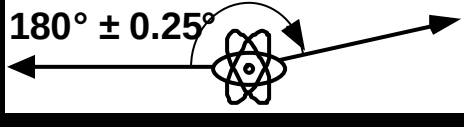

***Contribution* = 0.0022 D**
(D Detector Ring Diameter in mm)

- b^+e^- **Has Kinetic Energy (Not at Rest in Lab Frame)**
- **Emitted 511 keV Gammas are Not Back-to-Back**
- **Contribution Depends on Detector Ring Radius**
  (1.8 mm for 400 mm Whole Body PET,
  0.44 mm for 100 mm Animal PET)

Coding error:
Multiple penetration

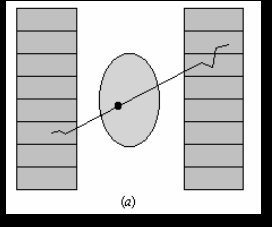

Coding error: Parallax

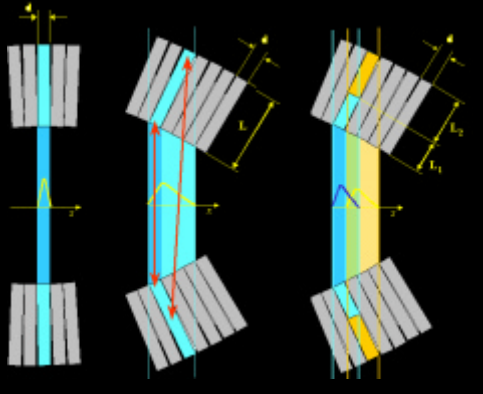

Penetration of 511 keV photons into crystal blurs measured position.

Blurring worsens as detector's attenuation length increases.

$$FWHM = 1.2\sqrt{(d/2)^2 + b^2 + (0.0022D)^2 + r^2 + p^2}$$

Crystal, Coding: *Intrinsic*; Non-colinearity; Positron range; Parallax error

1.2 : degradation due to tomographic reconstruction

d : crystal size

b : systematic inaccuracy of positioning scheme (range: 0-2 mm)

D : coincident detector separation

r : effective source size, including positron range 0.55mm w/ ^{18}F)

p : Parallax error (radial elongation)

***** Derenzo & Moses, "Critical instrumentation issues for resolution <2mm, high sensitivity brain PET", in *Quantification of Brain Function, Tracer Kinetics & Image Analysis in Brain PET*, ed. Uemura et al, Elsevier, 1993, pp. 25-40.

Scintillation timing

The light output from a scintillator is then proportional to the energy lost by the gamma ray.

The light is not emitted in one-shot but it follows an exponential decay behaviour due to the statistical de-excitation of the atoms with a τ between few tens up to few hundreds of ns.

The "speed" of the decay is critical in PET where a fast event discrimination is required for the coincidence.

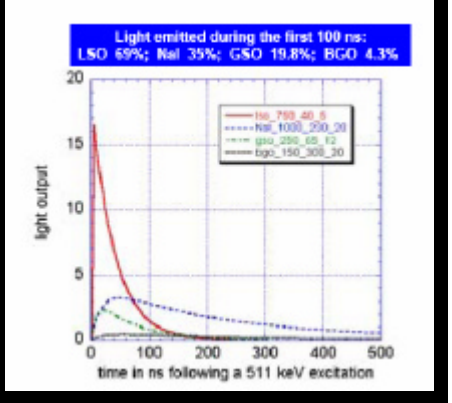

PET scintillators

❖ Detectors are usually scintillators :
the most often used is BGO (Bismuth germanate, $Bi_4Ge_3O_{12}$) and
more recently LSO (Lutetium Oxi-orto Silicate (LuSiO).

Material	Density [g/cm^3]	Atomic numbers	Light yield [%NaI(Tl)]	Decay time [ns]	Peak wavelength [nm]	Time resolution [ns]	Index of refraction	Comments
NaI(Tl)	3.76	11,53	100	230	410	1.5	1.85	Hygroscopic Low density
BGO	7.13	83,32,8	15	300	480	7	2.15	Low light yield Slow
LSO	7.4	71,32,8	75	40	480	1.4	1.82	Intr. background 400 cps/cm^3
GSO	6.71	64,32,8	26	600	430	-	1.85	Low light yield Slow
CsI(Tl)	4.51	55,53	45	1000	565	-	1.80	Slow
YAP:Ce	5.37	39,13,8	55	27	370	1.1	1.95	Medium Z

The Nobel Prize in Chemistry 2006

"for his studies of the molecular basis of eukaryotic transcription"

Photo: L. Cicero/Stanford University

Roger D. Kornberg

USA

Stanford University
Stanford, CA, USA

The Nobel Prize in Physiology or Medicine 2006

"for their discovery of RNA interference - gene silencing by double-stranded RNA"

Photo: L. Cicero/Stanford

Andrew Z. Fire

1/2 of the prize

USA

Stanford University School of Medicine
Stanford, CA, USA

Photo: R. Carlle/UMMAS

Craig C. Mello

1/2 of the prize

USA

University of Massachusetts Medical School
Worcester, MA, USA

"From man to mouse..."

- Most human genes have a related mouse gene: mice can be used as a platform for simulating many human diseases.
- Technological knowledge for producing different types of transgenic mice.
- Rats are the preferred animals for studies on neuroscience.
- Possibility of non-invasive studies on the same animal:
  - reduction in the number of sacrified animals
  - each animal can serve as its own control: less variability
- Bridge from animal to human research and to the clinic

	PROS	CONS
Clinical tomograph	**Available, Validated, Large Field Of View**	**Low Resolution and Low Sensitivity**
Dedicated instruments	High resolution and sensitivity	Validation of new detector concepts is needed (*new* scintillators, readout schemes, light sensors, etc.)

To fulfill the spatial resolution and sensitivity requirements, dedicated instruments are necessary.

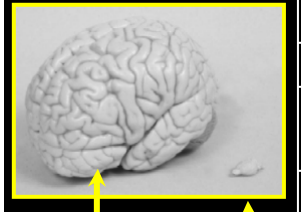

Human Rat

	Man	Rat	Mouse
Body weight	~70 kg	~200 g	~20 g
Brain (cortex apex-temporal lobe)	~105 mm	~10 mm	~6 mm
Heart	~300 g	~1 g	~0.1 g
Aorthic cannula (∅)	~ 30 mm	1.5 – 2.2 mm	0.9 - 1.3 mm

Required spatial resolution:

- Small size detectors (high pixellization)
- Individual detectors or "perfect" coding

6 mm FWHM (200 mm^3)

2 mm FWHM (8 mm^3)

≤ 1 mm FWHM (≤ 1 mm^3)

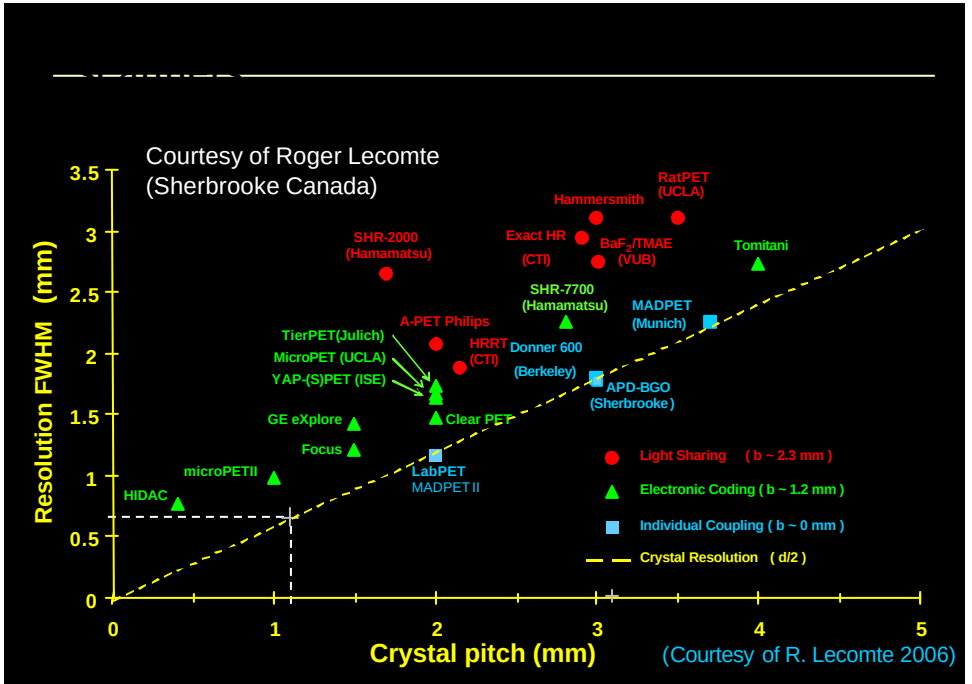
Courtesy of Roger Lecomte
(Sherbrooke Canada)
Resolution FWHM (mm)
Crystal pitch (mm)
3.5
3
2.5
2
1.5
1
0.5
0
0
1
2
3
4
5
RatPET
(UCLA)
Hammersmith
SHR-2000
(Hamamatsu)
Exact HR
(CTI)
BaF2/TMAE
(VUB)
Tomitani
SHR-7700
(Hamamatsu)
MADPET
(Munich)
A-PET Philips
TierPET(Julich)
MicroPET (UCLA)
YAP-(S)PET (ISE)
HRRT
(CTI)
Donner 600
(Berkeley)
APD-BGO
(Sherbrooke)
GE eXplore
Clear PET
Focus
LabPET
MADPET II
microPETII
HIDAC
Light Sharing (b ~ 2.3 mm)
Electronic Coding (b ~ 1.2 mm)
Individual Coupling (b ~ 0 mm)
Crystal Resolution (d/2)
(Courtesy of R. Lecomte 2006)

The Block Detector

1984-1985

Burnham, Brownell and colleagues at MGH developed a technique where scintillators were placed on a circular lightguide with photomultipliers placed on the opposite side of the lightguide. Charlie Burnham demonstrated that by taking the ratio of two adjacent photomultiplier signals, the scintillator that detected the gamma ray could be identified.

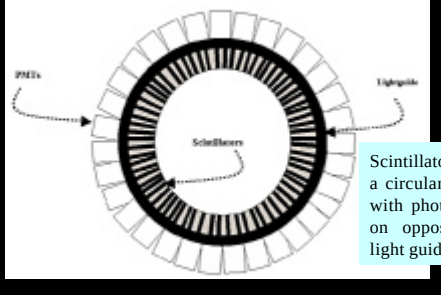

Scintillators placed on a circular light guide with photomultipliers on opposite side of light guide.

The block detector

Mike Casey and Ronald Nutt, from CTI, introduce the "Block" detector that was conceived as a means to simplify the Burnham detector and to make it easier to manufacture. Almost all dedicated tomographs built since 1985 have used some forms of the Block detector. This invention has made possible high-resolution PET tomographs at a much-reduced cost.

From the block detector to PS-PMT's

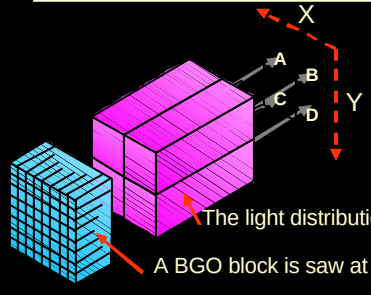

Center of gravity calculation for X and Y

$$X = \frac{(A+C)-(B+D)}{A+B+D+C}$$

$$Y = \frac{(C+D)-(A+B)}{A+B+D+C}$$

The light distribution is measured by 4 PMTs

A BGO block is saw at different depth.

Identification from a LUT

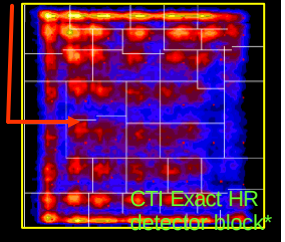

A position sensitive PMT is used for the readout of the matrix

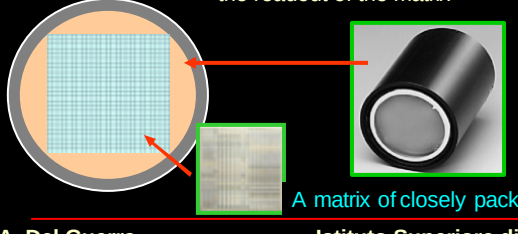

A matrix of closely packed finger crystals

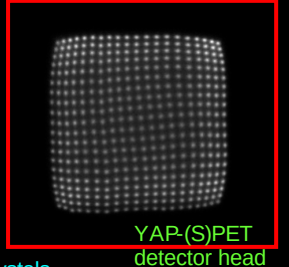

"light sharing" technique:
Hybrid position sensitive APD

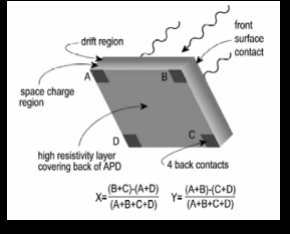

Picture of a HPS-APD with four output connectors

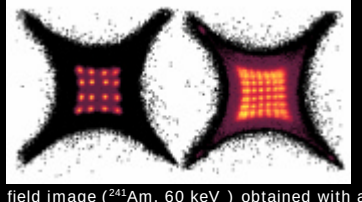

Flood field image (^{241}Am, 60 keV) obtained with a 4x4 and 8x8 CsI(Tl) scintillating matrices

"light sharing" technique:
Multi Anode flat panel PMT

MA-PMT (8×8 ch's)
Hamamatsu H8500
Active area 49 mm x 49 mm

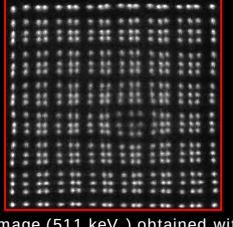

Flood field image (511 keV) obtained with a 20x20 YAP:Ce scintillating matrix (resistive readout)

APD

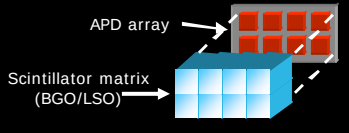

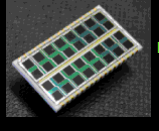

Implemented on MADPET II

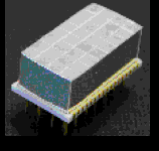

+ High spatial resolution
+ No Pile-up
+ No scattering in the crystals
- Expensive
- Many channels
- Difficult tuning

The detector module is composed by a matrix of 8×4 LSO crystals readout by a Hamamatsu S8550 (*Pichler B., IEEE TNS 45 (1998) 1298-1302)*

SiPM

SiPM are p-n diodes operating in **Geiger mode**, which means that the bias voltage is above the diode breakdown voltage.

In this way output is independent from input:
⇨ the surface is divided into **cells** (~1000/mm²)

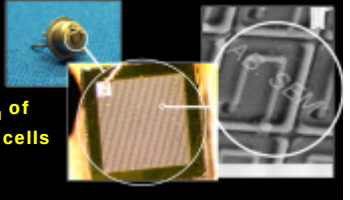

Signal μ N_{cell} **of hit cells**

+ High gain
+ Low noise
+ Good proportionality if $N_{photon} < N_{cell}$

An array of SiPMs can be used for "individual" readout, instead of PSMPT

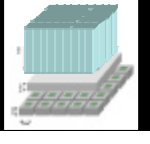

1-) Requirements

- Imaging of low activity sources:
  low uptake processes such as in gene research
- Possibility to study fast metabolic processes:
  characteristic time comparable with the scanning time

2-) Biological limitations

- Brain receptor saturation:
  usually a maximum of 100 microCi can be injected into a mouse
- Limitation on the volume
  a maximum of 300 microliters can be injected into a mouse

3-) Solutions

- Utilization of radionuclides with a very high specific activity
- High geometry efficiency: large solid angle covered by detectors
- High detection efficiency (e.g. for crystals: high/medium Z, high density)

Stationary ring geometry

Rotating planar geometry

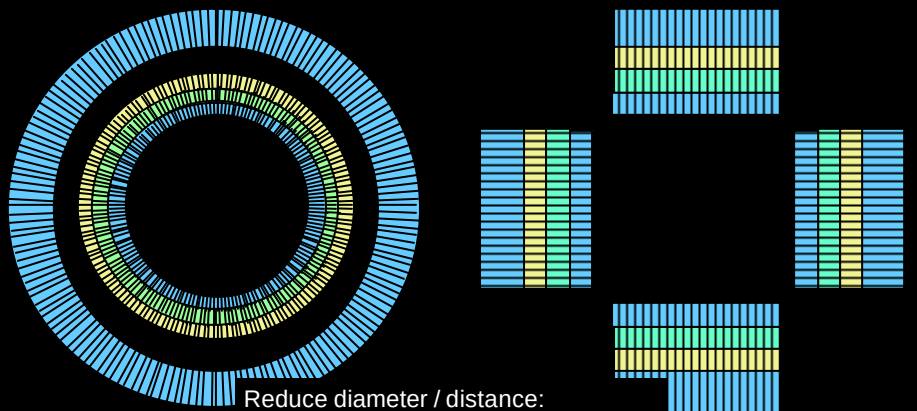

Reduce diameter / distance:

- Increase solid angle coverage
- Less crystals
- Thinner crystals

Increase thickness with DOI capability for increasing sensitivity for reducing parallax error

- Thick scintillator for high
- Radial elongation due to

high efficiency

ngation due to parallax error

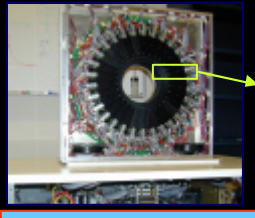

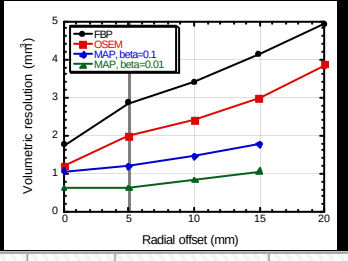

Specification (microPET II)

Scintillator:	14 × 14 LSO crystal array 90 detector modules in 3 rings 17640 LSO detector elements (0.95x0.95x12.5 mm each)
Inner diameter:	16.0 cm
Axial FOV:	4.9 cm
Transaxial FOV:	8.0 cm
Custom built gantry:	62 × 62 cm
Number of LORs:	51,861,600
# sinograms (3D):	1764
# image planes:	83
3D dataset size:	200 MB
Spatial resolution:	~1.2 mm @CFOV
Sensitivity:	~2.5%

microPET	resolution	Absolute Sensitivity	Animal Port
Focus$_{TM}$ 220	<1.3mm	>4.0%	22-26cm
Focus$_{TM}$ 120	<1.3mm	>7.0%	12-15cm

Courtesy of S. Cherry, UCLA, 2002

SIEMENS –CTI
microPET FOCUS

HIDAC: **HI**gh **D**ensity **A**valanche gas **C**hamber

(multi-wire proportional gas chamber with the addition of a conversion/multiplication structure)

Specifications	**Quad HIDAC**
FOV	28cm × 17cm Ø
No. of Detectors	4
No. of Chambers for each detector	8
Absolute Sensitivity	18cps/kBq
Resolution at Center	1.05 × 1.0 × 1.04 mm^3
Reconstruction	BPF, 3DRP, OSEM, ROPLE

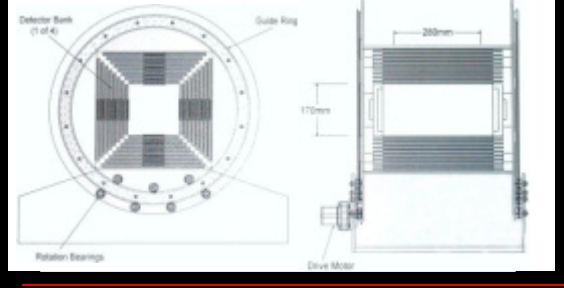

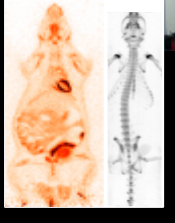

Left: Rat 18F-FDG scanning
Right: bone scanning after the injection of 17MBq of ^{18}F (OSEM reconstruction)

Differential measurement DUAL APD

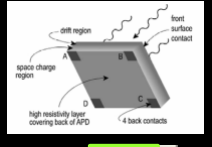

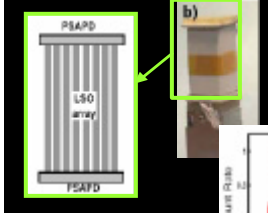

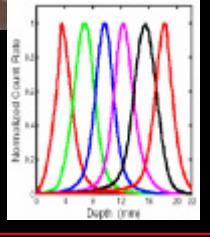

Resolution DOI measurement: 3 mm FWHM

Burr et al, *IEEE NSS/MIC* 2003

Differential measurement SiPD-PMT

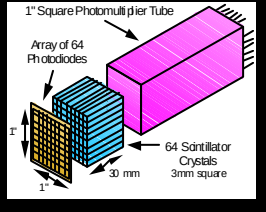

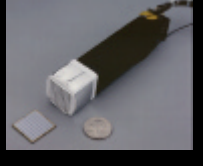

- The PMT (single anode) provides the timing
- The SiPD (8x8) detects the crystal
- The ratio SiPD/(SiPD+PMT) returns the DOI

“Pulse Shape” discrimination
“Phoswich detector”

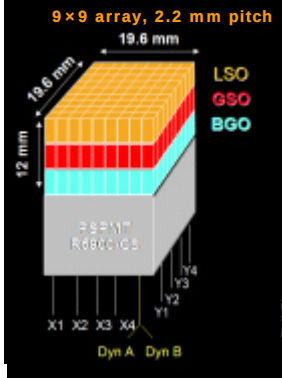

Used in the GE Xplore

Used in the ClearPET (LYSO/LuYAP)

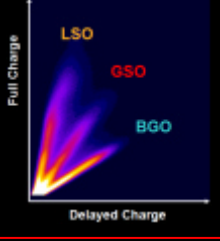

Seidel et al, *IEEE TNS* 46 (1998) 485

“Light coding”

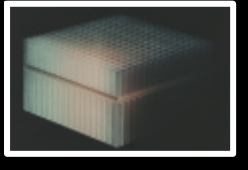

Implemented on ANIPET (Montreal)

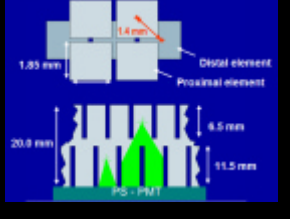

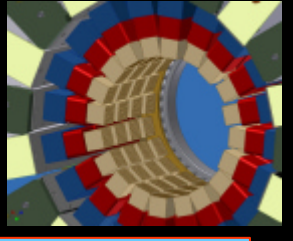

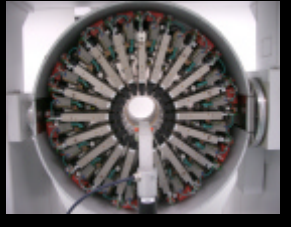

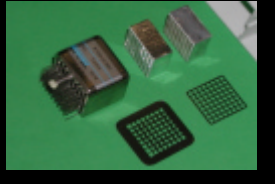

Geometry and dimensions

- inner diameter 140 mm
- animal port 120 mm
- 20x4 PM's in a ring
- axial shift for alternative PM row
- axial sensitive area 130 mm

The ClearPET detector module

Hamamatsu R7600 M64, multichannel PMT
64 LYSO:Ce crystals measuring 2x2x10 mm each
64 LuYAP:Ce crystals measuring 2x2x10 mm each

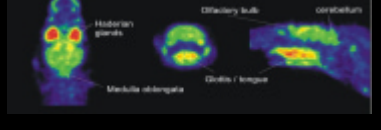

System performance

Maximum sensitivity@CFOV	3.05%
radial resolution @CFOV	1.32 mm
tangential resolution @CFOV	1.82 mm

Resolution	~1.2 mm (intrinsic) ~1.35 mm *or* 2.4 µl
Efficiency	1000 cps/µCi (2.6%)
Peak NEC	> 2500 kcps

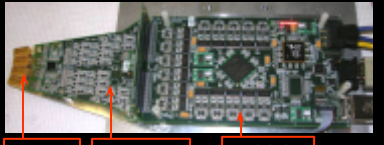

- 8-pixel, quad-APD detector module
- $2 \times 2 \times 10$ mm³ LYSO/LGSO scintillators
- 16-ch, 0.18 µm CMOS ASIC preamp
- Parallel, digital signal processing
- Real time list-mode data sorting
- High count rate, negligible deadtime
- User-friendly, ergonomic design

Scanner configuration

Configuration:	Four rotating heads
Scintillator:	$YAlO_3$:Ce (YAP:Ce)
Crystal size:	27 x 27 (1.5 x 1.5 x 20 mm^3 each)
Photodetector:	Position Sensitive PMT
Readout method:	Resistivechain (4 channels)
FoV size:	4 cm axial × 4 cm Ø
Collimators: (SPECT)	Lead (parallel holes)
Head-to-head distance:	10 cm

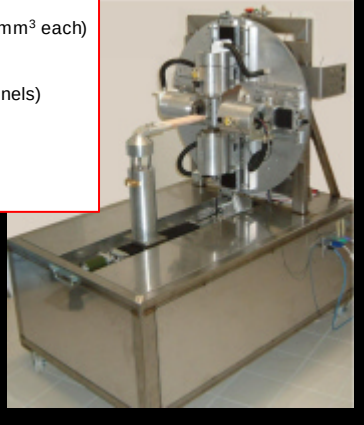

Material	Density [g/cm^3]	Atomic numbers	Light yield [%NaI(Tl)]	Decay time [ns]	Peak wavelength [nm]	Index of refraction	Comments
NaI(Tl)	3.76	11,53	100	230	410	1.85	Hygroscopic Low density
BGO	7.13	83,32,8	15	300	480	2.15	Low light yield Slow
LSO	7.4	71,32,8	75	40	480	1.82	Intr. background 400 cps/cm^3
GSO	6.71	64,32,8	26	600	430	1.85	Low light yield Slow
CsI(Tl)	4.51	55,53	45	1000	565	1.80	Slow
YAP:Ce	5.37	39,13,8	55	27	370	1.95	Medium Z

Good light yield
(critical for low energy photons in SPECT)
↓
Easier pixel identification and better energy resolution

Fast decay time
(critical for PET)
↓
excellent timing performance

Low photofraction
(4.4% @ 511 keV)

Why YAP (medium Z) for PET?

(Yttrium Aluminum Perovskite activated by Cerium)

Energy spectrum in a YAP:Ce block (4×4×3 cm^3)

Experimental

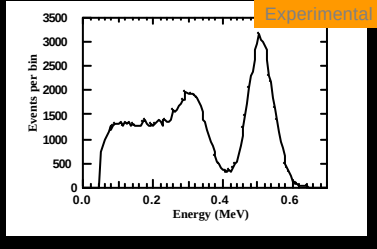

Monte Carlo

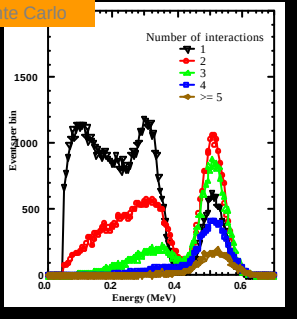

Selecting the **whole spectrum** (instead of photo-peak only) **single interactions** **(i.e. first interactions)** are privileged (about 65%) whilst other scintillators have a photofraction below 50%.

⇒ **Higher sensitivity**

Selecting the events with an energy deposit **below 400 keV (Compton only)** mainly **first interactions** are considered ⇒ Better **point of interaction** reconstruction (center of mass calculation)

⇒ **Higher spatial resolution**

- AmbiSEN Center of excellence, University of Pisa, I
- University of Ferrara – Institute of Nuclear Medicine, I
- CEINGE – University of Naples, I
- San Raffaele Hospital – Milan, I
- ACOM Advanced Oncology Center, Macerata, I
- Archamps Technobiopark, F

Transaxial sections (0.25 mm x 0.25 mm x 2.0 mm)

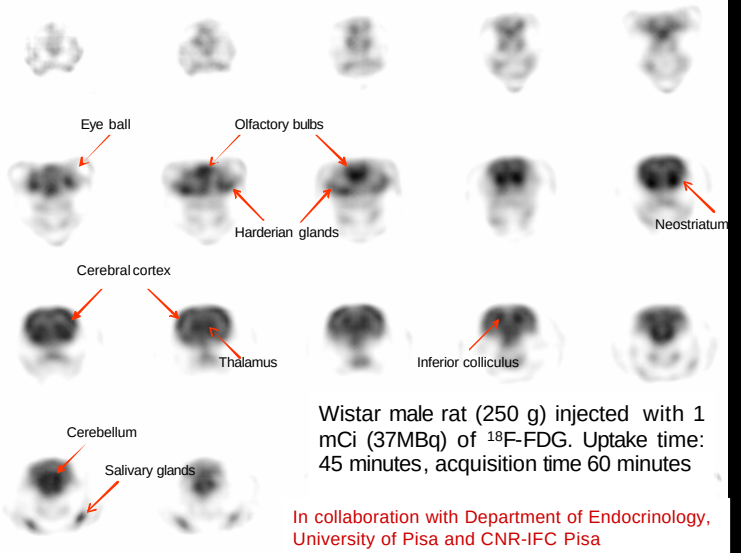

Wistar male rat (250 g) injected with 1 mCi (37MBq) of ^{18}F-FDG. Uptake time: 45 minutes, acquisition time 60 minutes

In collaboration with Department of Endocrinology, University of Pisa and CNR-IFC Pisa

Pentobarbital

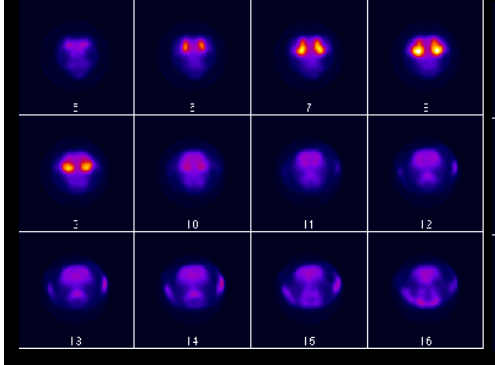

23.5 MBq injected,
uptake time 30 minutes, acquisitions 30 minutes,
EM reconstruction (10 iterations)

Tribromoethanol

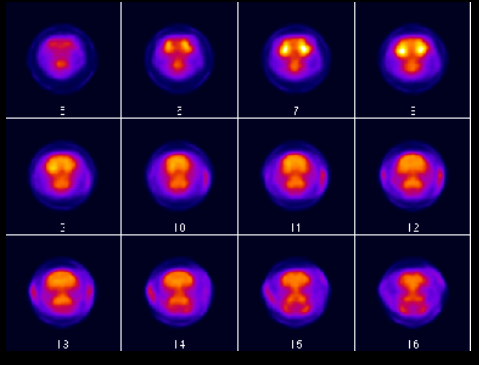

29.6 MBq) injected, uptake time 38 min,
acquisitions time 30 min,
EM reconstruction (10 iterations)

In collaboration with HSR S. Raffaele, Milano, Italy

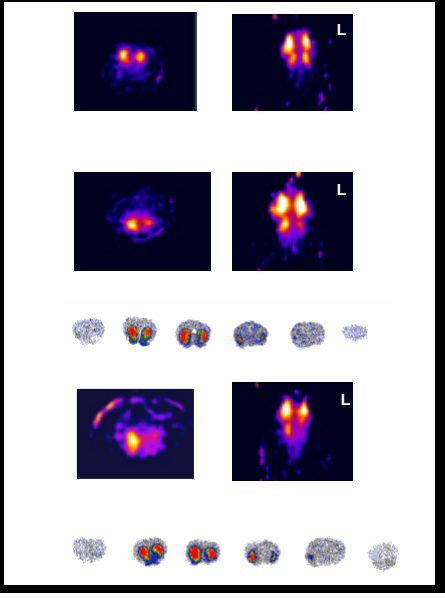

Evolution of a monolateral lesion QA induced

Surgery

Male Wistar rats weighting 300 g were injected icv in the left striatum with 210 nmol of QA solution and in the right striatum with PBS 0.1 mol/L. Stereotaxic coordinates: AP=+ 1.5, L=+ 2.6, V=-7.0 mm from the Bregma, according to the atlas of Paxinos and Watson.

Autoradiography

Eight and thirty days after the surgery respectively, two rats were injected with 130 µCi of [^{1}C]Raclopride and sacrificed after 30 minutes. The brain was rapidly removed and coronal section of 2 mm-thickness were performed on unfrozen tissue using a brain matrix. Acquisition for 100 minutes with Cyclone Storage Phosphor System .

In collaboration with HSR S. Raffaele, Milano, Italy

YAP-(S)PET animal imaging

Oncology: F98 tumor bearing rat (PET).

Normal rats (Wistar) were compared with rats with a brain glioma in terms of brain glucose consumption (FDG). The technique is able to identify the size and the position of the tumor in the brain.

Control Rat

Rat with brain glioma

3D-rendering, maximum projections

In collaboration with CNR-IFC Pisa

YAP-(S)PET animal imaging: Perfusion in the myocardium with ^{99m}Tc-Myoview (SPECT).

Sprague-Dawley male rat (204 g) Injected activity 300 MBq of ^{99m}Tc Myoview
Scan time: 80 min. (180 min. post injection)

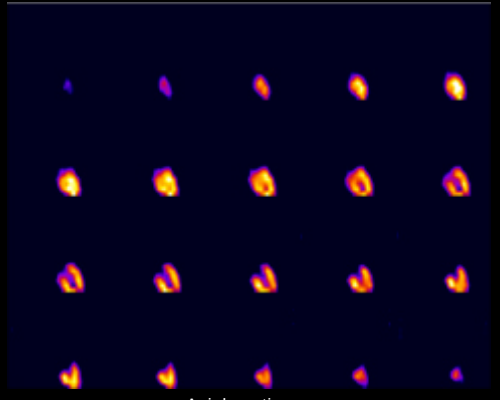

Axial sections
(0.5 x 0.5 x 0.5 mm voxel)

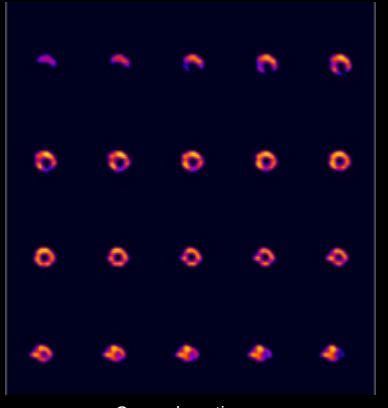

Coronal sections
(0.5 x 0.5 x 0.5 mm voxel)

In collaboration with CNR-IFC Pisa

PET modality

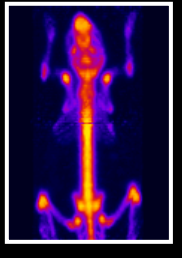

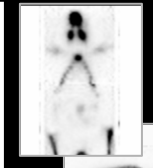

Longitudinal sections

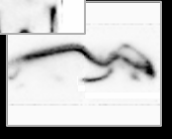

Mouse (200 g) injected with 2 mCi (74 MBq) of $^{18}F^-$. Uptake time: 2 hours, acquisition time 1 hour (2 bed positions).

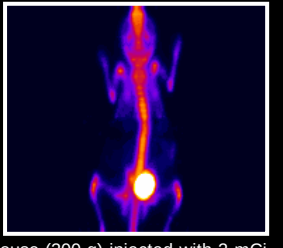

Mouse (200 g) injected with 2 mCi (74 MBq) of NaF. Uptake time: 2 hours, acquisition time 1 hour (2 bed positions).

In collaboration with Oncodesign,Dijon, France

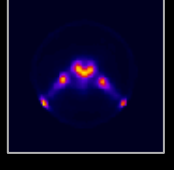

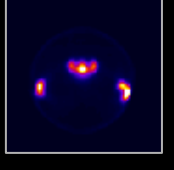

Transaxial slices (2 mm thick)

In collaboration with University of Mainz, Germany

SPECT modality

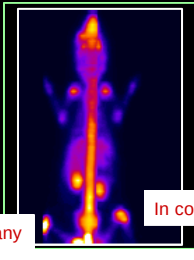

Mouse injected with 10 mCi (370 MBq) of ^{99m}Tc-MDP. Uptake time: 2 hours, acquisition time 82 minutes (3 bed positions).

In collaboration with University of Ferrara, Italy

- A single detector head with multiple layers of scintillator
- Continuous slabs of crystal viewed by a large number of SiPMs

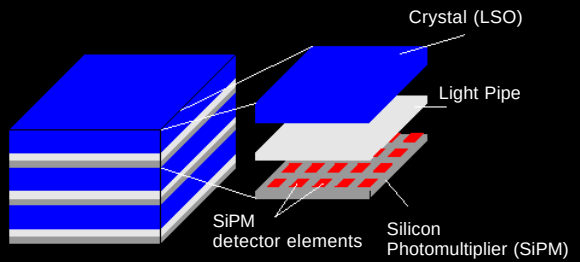

"A small-animal PET design using SiPMs and Anger Logic with intrinsic DOI"

S. Moehrs et al., Univeristà di Pisa. Presented at IEEE-NSS-MIC 2004

Whole Scanner:

2 or 4 rotating detector heads

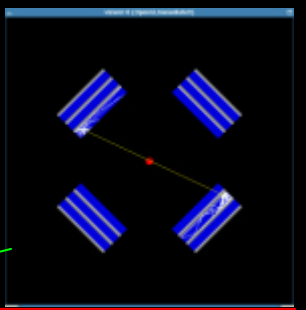

Geant 4 Simulation

For a single detector head with 3 x 5 mm LSO, and no light pipe we obtain for 511 keV gamma rays

- An efficiency of ~70 %
- An intrinsic detector resolution of ~0.4 mm (in the center of the detector)

Intrinsic detector spatial resolution and displacemente error for 511 keV gamma rays over the detector head surface:

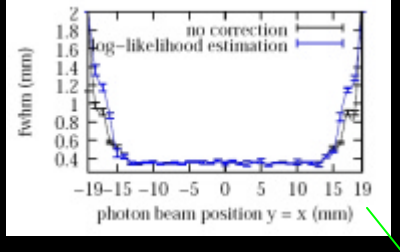

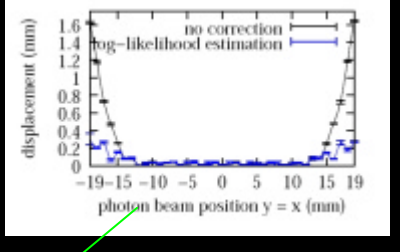

Dedicated correction method should be applied to improve the performance towards the edges of the detector

The **SiliPET** small animal PET scanner is composed by 4 detector stacks each composed of 40 planar, 1 mm thick, **double sided silicon strip detectors** with 128 strips on each side to permit the measurement of the two coordinates on the plane of the detector.

The third coordinate, the depth of interaction, is given by the identification of the detector plane in which the interaction takes place with a precision determined by its thickness.

All planes in a stack are in ***exclusive OR*** imposing therefore a single interaction.

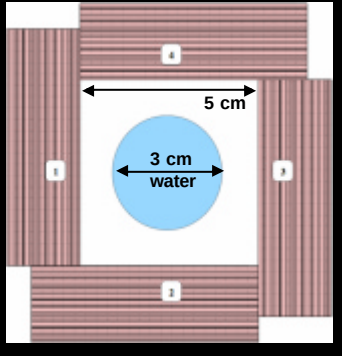

- ***Stack layer*** → **DOI mesurement**
- ***Compton interaction*** → **accurate position**
- ***No parallax*** → **compact and high sensitivity**
- ***No energy mesurement*** → **no ADCs**

Simulation ingredients

Emitted positrons with ^{18}F spectrum.
Included non collinearity of gamma rays.
Each detector subdivided in cells.
Electron transport included.

Spatial resolution: sinogram profiles

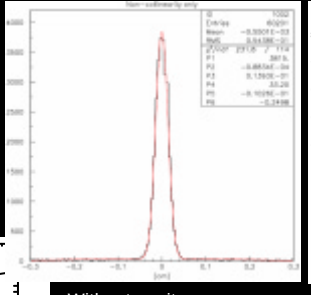

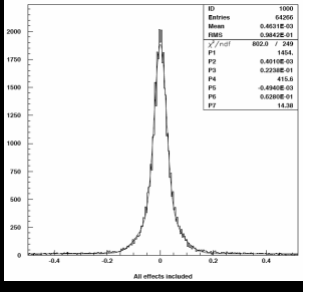

Without positron range,
FWHM = 0.33 mm
due to strip pitch

Including positron range,
FWHM = 0.52 mm

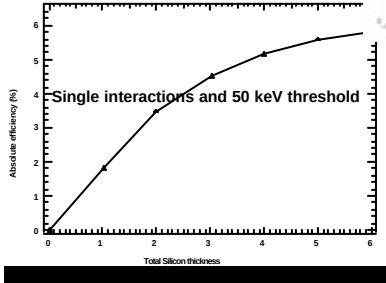

5.1% absolute efficiency for
a stack thickness of 4 cm

Mesurements with a ~ 1 mm diameter ^{22}Na source. The MEGA detector was devided into two stacks 2 cm apart made by of 5 and 6 prototype layers.
Coincidence events between top and bottom stacks were taken and logical XOR for layers in each stack was implemented.
Due to the 1 micosecond time window (MEGA electronics) a low activity source was used to keep random coincidences low.

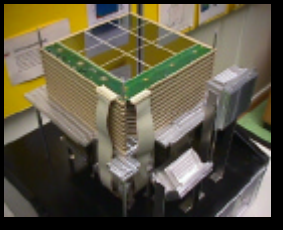

MEGA prototype tracker: 11 doublesided Si 19 X 19 cm^2 detector layers. Si wafer parameters: thickness = 0.5mm; strip pitch = 470 microns.

Composition of reconstructed with a focal plane ray-tracing method images of the source acquired in different positions.

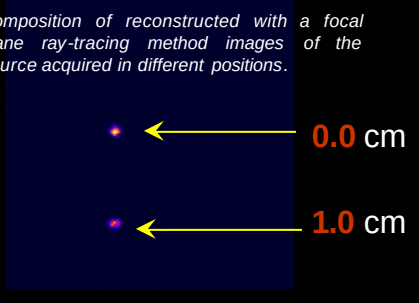

Profile through the sources of the composite image. FWHM = 0.75 mm. Souce diameter = 1 mm. Same results are obtained by simulating a uniform1 mm diameter sphere.

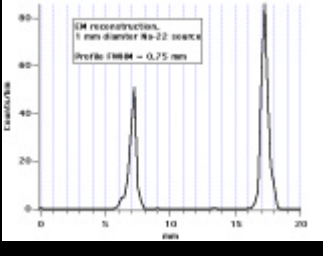

X-ray CT instrumentation

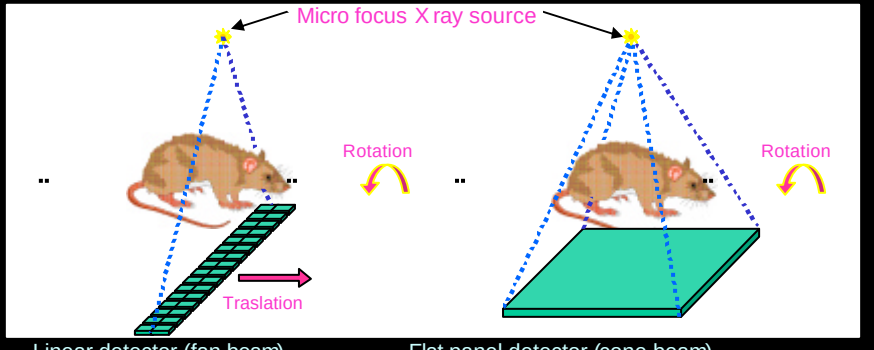

Linear detector (fan beam)
Recon.: Filtered Back-Projection (FBP)

Pro's: Detector cost
Easy image reconstruction

Con's: Traslation required
Scanning duration
X-ray collimator is required

Flat panel detector (cone beam)
Recon.: Feldkamp Filtered Back-Projection (FBP)

Pro's: FOV, no traslation required
Fast scanning

Con's: Reconstruction complexity

Photodetector: scintillator or phosphor screen coupled to CCD or CMOS or semiconductor (e.g. a-Se)

Small animal CT @ Pisa University

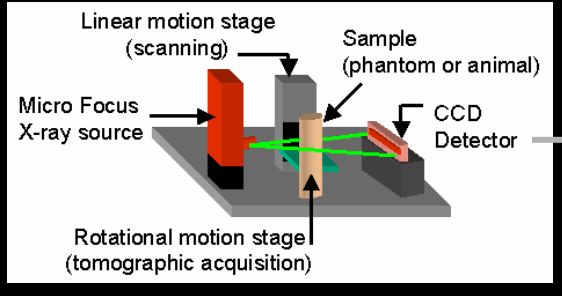

Schematic representation of the small animal CT prototype.

Hamamatsu S7199 (Fiber optic plate + scintillator (CsI) coupled to a CCD)

Experimental setup at INFN - University of Pisa

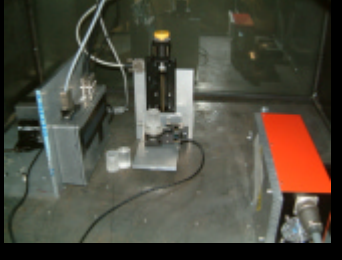

Expected CT performance

Spatial resolution	100-200μm FWHM
Coefficient of variation (s_m/m)	6% @ 80mm voxel

Single photon counting detector

1 mm thick silicon pixel detector bump-bonded to the Medipix2 chip.

The detector is a matrix of 256 x 256 square cells, with 55 µm side.

The active area is 14 x 14 mm^2

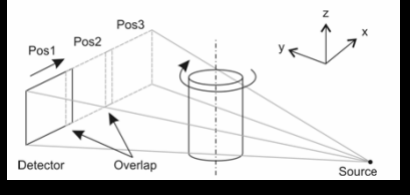

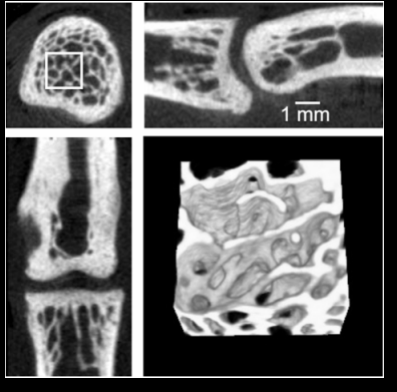

Tomographic images of the finger joint of a chicken: transaxial (top-left), sagittal (top-right) and coronal (bottom-left). The 3D visualization (bottom-right) corresponds to the highlighted zone in the transaxial image. In the images above, the voxel is a cube of 30 µm. Typical thickness of trabeculae is 50-100 mm.

Two independent scanners share the same animal bed.
The X-ray tomography obtained with the CT scanner is followed by
a PET scan or viceversa

CT

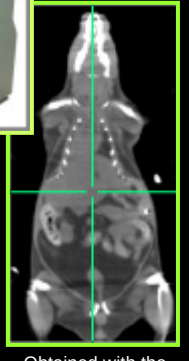

Obtained with the
ImTEK CT scanner

PET

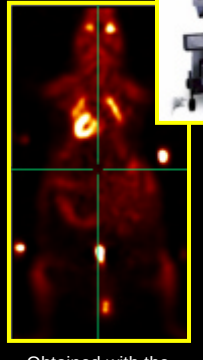

Obtained with the
MicroPET scanner

FUSED!

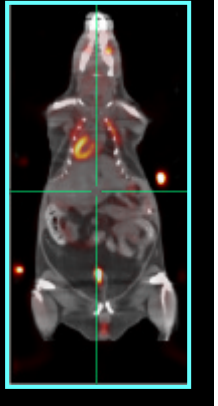

Concept: two opposing heads in PET mode and two heads in SPECT mode

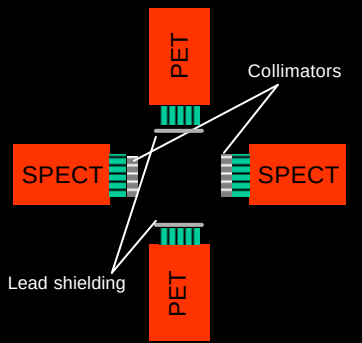

- 2 mm lead shields PET detectors from 140keV γ's
- SPECT detectors are in XOR
- Energy selection window for SPECT events

Possible with the YAP-(S)PET scanner

Experimental proof of principle with YAP-(S)PET: simultaneous PET/SPECT tomography

PET: 18μCi SPECT: 840μCi

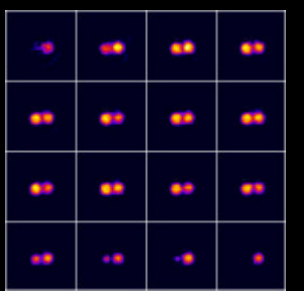

PET and SPECT together

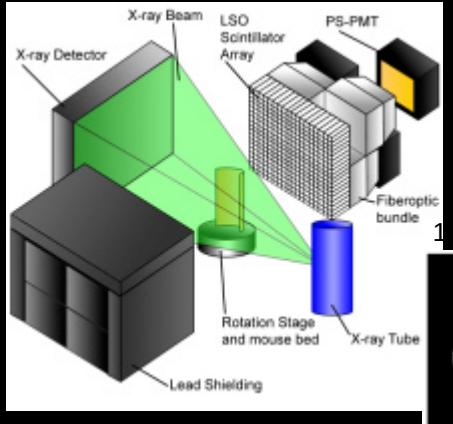

Courtesy of S. Cherry, UCLA, 2002

- Minifocal x-ray tube
- a-Se CMOS digital x-ray detector
- LSO plate detectors for PET
- Simultaneous PET and CT acquisition

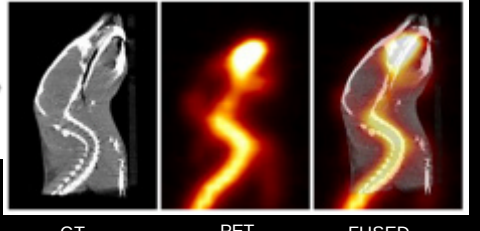

CT PET FUSED

❖ **Center of Excellence AmbiSEN** (Molecular imaging)

Prof. Aldo Pinchera Dip. Endocrinologia e Metabolismo, Ortopedia e Traumat. Medicina del Lavoro
Prof. Amedeo Alpi Dip. Biologia delle Piante Agrarie
Prof. Roberto Barale Dip.Scienze dell'Uomo e Ambiente
Prof.ssa Giuseppina Barsacchi Dip.Fisiologia e Biochimica
Prof. Giovan Battista Cassano Dip.Psichiatria, Neurobiologia, Farmacologia, e Biotecnologie
Prof. Giovanni Umberto Corsini Dip. Neuroscienze
Prof. Alberto Del Guerra Dip. Fisica "E.Fermi"
Prof. Antonio Lucacchini Dip.Psichiatria, Neurobiologia, Farmacologia, e Biotenologie
Prof. Luigi Murri Dip. Neuroscienze
Prof. Piero Salvadori Dip. Chimica e Chimica Industriale
Prof. Giulio Soldani Dip. Clinica Veterinaria

❖ **Department of Nuclear Medicine and Oncology, University of Pisa** (PEM)
❖ **ISE – Ingegneria dei Sistemi Elettronici** (small animal PET/SPECT)
❖ **CNR Prof. Luigi Donato** (small animal PET/SPECT)
❖ **Università di Ferrara** (small animal PET/SPECT)
❖ **IRCCS "Stella Maris"** (fMRI)
❖ **Università di Erlangen Prof. W. Kalender** (small animal CT)
❖ **University of Mainz Prof. Frank Roesch**
❖ **Ospedale S. Raffaele (Milano) Prof. F. Fazio** (small animal PET/SPECT)
❖ **EMIL (European Molecular Imaging Laboratory) – FP6 NoE**

Functional Imaging and Instrumentation Group at Pisa

Home «««
Research
People
Publications
Positions
Contact
Links

Alberto Del Guerra
Nicola Belcari
Antonietta Bartoli
Gina Belmonte
Walter Bencivelli
Laura Biagi
Manuela Camarda
Serena Fabbri
Judy Fogli
Stefania Linsalata
Gabriela Llosa Llacer
Sara Marcatili
Sascha Moehrs
Daniele Panetta
Michela Tosetti
Sara Vecchio

www.df.unipi.it/~fiig